In vivo imaging of immediate early gene expression reveals layer-specific memory traces in the mammalian brain

Hong Xie, Yu Liu, Youzhi Zhu, Xinlu Ding, Yuhao Yang, and Ji-Song Guan[1]

Ministry of Key Laboratory of Protein Sciences, Tsinghua-Peking Joint Center for Life Sciences, Center for Epigenetics and Chromatin Biology, School of Life Sciences, Tsinghua University, Beijing 100084, China

Edited by Terrence J. Sejnowski, Salk Institute for Biological Studies, La Jolla, CA, and approved January 16, 2014 (received for review September 5, 2013)

The dynamic processes of formatting long-term memory traces in the cortex are poorly understood. The investigation of these processes requires measurements of task-evoked neuronal activities from large numbers of neurons over many days. Here, we present a two-photon imaging-based system to track event–related neuronal activity in thousands of neurons through the quantitative measurement of EGFP proteins expressed under the control of the EGR1 gene promoter. A recognition algorithm was developed to detect GFP-positive neurons in multiple cortical volumes and thereby to allow the reproducible tracking of 4,000 neurons in each volume for 2 mo. The analysis revealed a context-specific response in sparse layer II neurons. The context-evoked response gradually increased during several days of training and was maintained 1 mo later. The formed traces were specifically activated by the training context and were linearly correlated with the behavioral response. Neuronal assemblies that responded to specific contexts were largely separated, indicating the sparse coding of memory-related traces in the layer II cortical circuit.

In the mammalian brain, memory traces in cortical areas are poorly understood. In contrast to the medial temporal lobe, particularly the hippocampus, which is involved in the temporary storage of declarative memories (1, 2), the neocortex is believed to store remote memories (3–6). However, remarkably little knowledge regarding the sites and dynamics of remote memory storage has been revealed at the cellular level owing to the complexity of the connections and the large number of neurons within the cortical circuit.

In vivo electrophysiological recording of neuronal firing revolutionized neurobiology by linking neuronal activity with animal behavior. The small number of neurons recorded by the electrodes, however, was a limitation, as information coding and decoding may use an army of neurons forming neuronal assemblies (7, 8). Efforts to record the activity of larger populations of neurons in cortical volumes have been actively pursued by either increasing the number of electrode probes (7, 9–11) or using calcium indicator–based imaging (12–15) and immediate early gene (IEG)-based reporters (16–18). The expression of IEGs is correlated with the averaged neuronal activation on external stimuli (19, 20), implying that the marked neurons are involved in behavior (1, 21–25). Studies using in vivo imaging of IEGs have revealed cortical coding in the visual cortex and in other cortical areas, reflecting electrical activation in individual neurons (16, 17). Among IEGs, the expression of early growth response protein 1 (EGR1, also known as zif268) is associated with high-frequency stimulation and the induction of long-term plasticity during learning (26, 27). To measure neuronal activation in cortical circuits during a behavioral task, we used an EGR1 expression reporter mouse line in which the expression of the EGFP protein is under the control of the Egr1 gene promoter. We designed offline recording strategies to monitor task-associated neuronal activity by quantifying changes in cellular EGFP signals in the mouse cortex. Patterns of activated neuronal assemblies during different tasks were visualized in the entire cortical volume. Furthermore, through computer recognition-based reconstruction, we were able to track the activity-related cellular EGFP signals from multiple cortical areas for 2 mo to reveal memory-related changes in the cortical circuit.

Results

We first calibrated the neuronal activation-induced expression of EGR1-EGFP in vitro and in vivo. The protein and mRNA levels of EGFP reflect the expression of the Egr1 gene in the transgenic mice (Fig. S1). Although the EGFP protein was believed to be stable, the EGFP signals in cultured cortical neurons exhibited significant decay within one hour after the application of chemical blockers of synaptic transmission [MK801, CNQX or the sodium channel blocker tetrodotoxin (TTX)] (Fig. S2*A*). Conversely, enhancing the neuronal activation using dihydroxyphenylglycine (DHPG) triggered an increase in the EGFP signal within one hour. Therefore, the EGFP signals reflected neuronal activation in cultured neurons. To further characterize activity-dependent EGFP expression, we quantified the induction of EGFP in response to frequency-specific stimuli in cortical neurons transfected with channelrhodopsin-2 (ChR2). The expression of EGFP, which was measured 1 h after the stimuli, exhibited a highly positive correlation with the frequency of the light (Fig. S2*B*). Because the stimulation of ChR2-expressing neurons induces reliable neuronal firing at an identical frequency to the light stimuli (28, 29), this frequency-dependent EGFP expression suggested that the level of EGFP in neurons was related to the spiking intensity in the neuron one hour before the recording.

Next, we measured the cellular EGFP signal dynamics in the mouse visual cortex during visual stimuli. The EGFP signals were acquired using multiphoton imaging through a cranial window (30–32) (Fig. S2*C*). In the reporter line, the EGR1-EGFP signal

Significance

This study demonstrates how sensory information is represented and stored in cortical circuits during complex behavior in the mammalian brain. Using a newly established automatic algorithm for cell detection, we tracked the expression of immediate early genes from more than 20,000 neurons in each living mouse for 2 mo, revealing quantitative signal changes in each neuron within a local cortical circuit. A natural behavioral task induced sparse and task-specific neuronal activation in cortical layer II. The gradually formed sparse activation of neurons was observed in multiple cortical areas. Our results support the concept of consolidation for long-term memory storage in cortical circuits and demonstrate the representation of natural events as sparse coding in the mammalian brain.

Author contributions: H.X. and J.-S.G. designed research; H.X., Y.L., and X.D. performed research; H.X. and J.-S.G. contributed new reagents/analytic tools; H.X., Y.L., Y.Z., Y.Y., and J.-S.G. analyzed data; and H.X. and J.-S.G. wrote the paper.

The authors declare no conflict of interest.

This article is a PNAS Direct Submission.

[1]To whom correspondence should be addressed. E-mail: jsguan@mail.tsinghua.edu.cn.

This article contains supporting information online at www.pnas.org/lookup/suppl/doi:10.1073/pnas.1316808111/-/DCSupplemental.

could be detected using multiphoton microscopy at low laser power (7.8–12.5 mW). Time-lapse scanning indicated that light deprivation suppressed the cellular EGFP signal in the visual cortex with an exponential decay ($R^2 = 0.9967$, $n = 450$ cells from three mice; Fig. S2 *D* and *E*), indicating that the virtual half-life of the EGR1-EGFP protein in cortical neurons was approximately 2 h under anesthetic (Fig. S2*E*). In anesthetized mice, 10 min of stimulation using a 50-Hz flash (25 mW, LED, blue light) to the left eye induced a robust increase in the EGFP signal with a delay of approximately 1 h (Fig. S2 *F–H*). Based on the measured EGFP metabolism rate, the dynamics of the EGFP signals indicated that neuronal activation induced a sharp pulse expression of EGFP, which peaked 1 h after the stimulus (Fig. S2*G*). In contrast to the visual cortex, which was directly activated by visual stimuli, the motor cortex did not exhibit stimulus-induced EGFP expression in the same mice (Fig. S2*F*), indicating the specificity of this neuronal activity reporter. Owing to the temporal precision of activity-induced EGFP expression 1 h after the stimulus (Fig. S2*G*), this reporter system provided a unique opportunity to acquire neuronal activity-related signals in free-moving mice through the measurement of task-induced neuronal responses 1 h after behavioral training.

To further characterize the induction of EGFP expression by behavioral training in free-moving mice, we examined the relative changes in the cellular EGFP signals after contextual fear training in comparison with the home cage condition in the same mice (Fig. S3 *A* and *B*). Mice were anesthetized (isoflurane) immediately after training to eliminate posttraining activities and thereby to ensure that the neuronal activation difference between the home cage trial and the training trial corresponded to the 3-min training. The cellular EGFP signals were significantly higher in the training trial than in the home cage trial at 55 min after anesthetization (Fig. S3*B*; $n = 3{,}323$ neurons), indicating that the training induced higher activity than the home cage trial. Quantification of the cellular EGFP signal changes revealed that the task-related EGFP expression reached a peak 55 min after training (Fig. S3*C*). Furthermore, the training-induced EGFP signals remained higher than the signals induced by the home cage trial for more than 1 h. The training-induced signal increase was specific, as the averaged cellular signal in two home cage trials did not change (Fig. S3*D*; $n = 3{,}633$ neurons). Therefore, the maintenance of activity-induced EGFP signals provided a 1-h time window for recording responses in multiple cortical regions to an identical training trial.

According to the characterization of the activity-related EGFP signals, we designed a standardized protocol to track task-related neuronal activation in multiple cortical regions (Fig. 1 *A* and *B*). The EGFP signals in the cortical volumes were recorded 1 h after each training trial (Fig. 1*C*). In each animal, we recorded five to six cortical volumes, each with a dimension of $339 \times 339 \times 300$ or $509 \times 509 \times 300$ μm, at 2-μm intervals in depth, which revealed a total of 2,500–4,500 EGFP-positive neurons in each volume.

To perform reproducible long-term recording in the cortical volume, we developed an automatic cellular EGFP signal detection algorithm to align and measure signals in each neuron within the circuit. Each image was screened through a learning algorithm (*Materials and Methods*, Dataset S1) to recognize each EGFP-positive neuron and to mark the centers of the cells (Fig. 1*D*). The computer recognition achieved a 90% correct rate for cell recognition (Fig. S4). This recognition process was further manually validated to add missing cells and to correct errors. The EGFP intensity in each cell was quantified around the center as the averaged intensity in a $12 \times 12 \times 6$-μm voxel. Each neuron was marked with a unique ID. The computer recognition system assisted in monitoring the activity-related EGFP signals in the cortical volume in the range of 4,000 neurons per volume (with a dimension of $509 \times 509 \times 300$ μm) under various tasks (Fig. 1*E*).

Using this reporter system, we began to test whether different behavior training in distinct contexts induced differential expression of EGR1-EGFP in specific neuronal ensembles. Because the

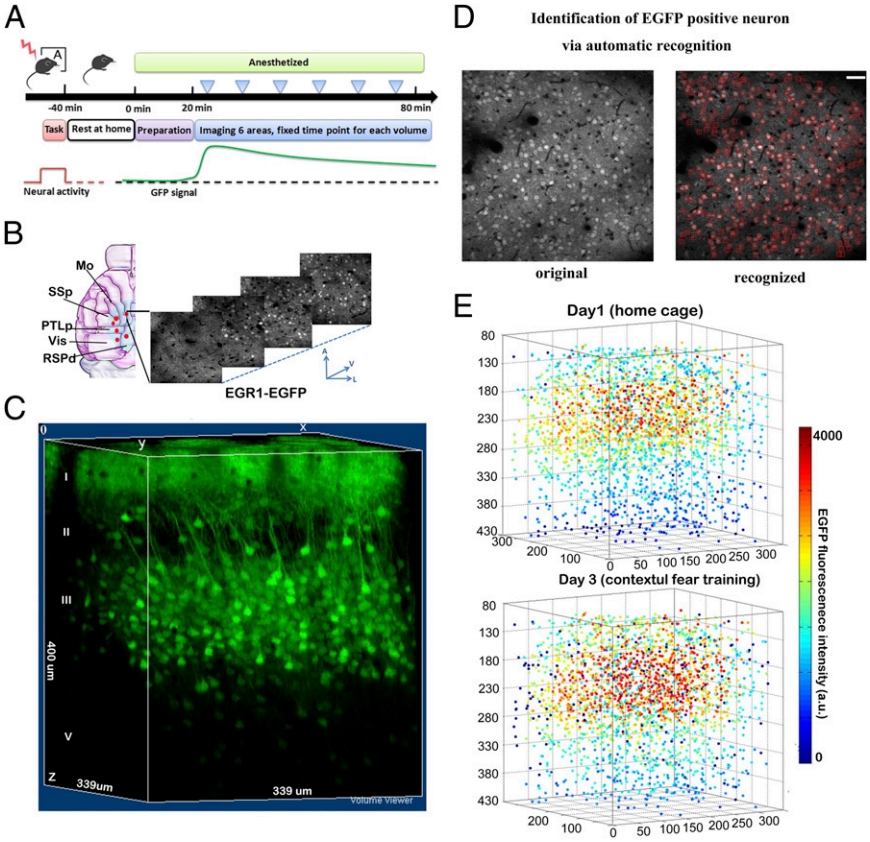

Fig. 1. Digitized reconstruction of the EGR1-EGFP signals to track neuronal activation in the same cortical volume on different tasks. (*A*) Standard experimental procedure to measure the task-induced EGFP signal in mice. Individual cortical volume was imaged at the same time point after the training for different trials to compare signal differences between behavior tasks. (*B*) Multiple cortical volumes were imaged within the blue area at the z-step of 2 μm. Vis, visual cortex; Mo, motor cortex; SSp, primary sensory cortex; PTLp, posterior parietal association; RSPd, dorsal part of retrosplenial cortices. A, anterior; V, ventral; L, lateral. (*C*) Example of the 3D reconstruction of the EGR1-EGFP signals in the motor cortex. Block size, $339 \times 339 \times 400$ μm. (*D*) The designed recognition system was used to identify the EGFP-positive neurons on each image according to their morphology pattern. The red squares showed the computer-recognized cells. The same cells identified in multiple optical sections were further filtered to obtain the center position of the cell. Detection errors were corrected manually after primary screening. (Scale bars, 50 μm.) (*E*) The example of digitized reconstruction of the cellular EGFP signals in a cortical volume for two trials ($n = 3{,}563$). Indexed color showed the EGFP fluorescent intensity.

environmental stimuli during a behavioral task changes from time to time, it was unclear whether there were specific and stable neuronal ensembles that responded only to a specific context. Cellular EGFP signals were imaged after behavior training in the same volume over 2 mo. To better illustrate the signal dynamics in distinct neuronal ensembles, EGFP expression in different tasks was labeled using pseudocolor (Fig. 2*A*). We found that most neurons exhibited overlapping EGFP expression induced by different tasks. Only a small group of neurons (0.1–0.3% in the entire volume) exhibited exclusive expression of EGR1 on different tasks. In the neurons with overlapped signals, the quantitative expression of EGFP also exhibited differences between specific tasks. The exclusive expression of EGR1 in different tasks within sparsely located neurons was primarily observed in the superficial layer of L2/3 neurons (~80–120 μm subpial), presumably in layer II (L2). Surprisingly, such context-specific responses were observed in all cortical areas, including the motor cortex, the visual cortex, the somatosensory cortex, and the retrosplenial cortex (Fig. 2*B*). The 3D reconstruction view of the visual cortex and the dorsal region of the retrosplenial cortex (RSPd) further confirmed the separation of the task-specific activities in layer II neurons (~100 μm below the pia mater; Fig. 2*C* and Fig. S5). In contrast, L4 neurons exhibited nonseparated activities in trials using different contexts (Fig. 2*C*). The differential expression of EGR1 in L2 neurons under different contexts was due to the context specificity, as an identical task evoked similar EGR1 expression in the L2 neuron ensemble (Fig. 2*D*). Therefore, contextual training induced specific responses in L2 neuron ensembles.

To test whether these context-specific responses were formed during learning for the specific task, we recorded the context-related EGR1 expression for 2 mo. The contextual fear conditioning training-induced EGFP signals were acquired by comparing the cellular EGFP signal in the training trial to the homecage trial (Fig. 3*A*). The task-induced signal above the baseline activity (ΔF) in the entire cortical volume exhibited a Gaussian distribution. Only a small fraction of neurons demonstrated significantly higher activation by the fear conditioning trial compared with the home cage trial (greater than 2.8-fold of the SD; Fig. S6). After multiple trials of contextual fear condition training in context A, the mice exhibited freezing behavior during recall trials in context A (Fig. 3*B*). A consistent population of neurons was identified as context A neurons during recall trials in context A at day 5 and day 12 (with an overlapping rate of 36.9 ± 5.2%, $n = 15$ volumes from three mice). The context-specific neuronal ensembles (memory traces) were identified as those neuronal ensembles that were commonly activated (>2.8-fold of the SD compared with the home cage trial) in both of the recall trials (Fig. 3*B*). We tracked the changes in the EGFP signals in each trial within these identified neuronal ensembles. Interestingly, the identified neuronal ensembles gradually acquired the context A–evoked activity during several days of the learning/consolidation process (Fig. 3 *C* and *D*), indicating that the response to context A in these cells was not a sensory response but a learned memory response (Fig. 3 *C* and *D*). In contrast to the identified neuronal ensembles, the averaged signals of all neurons in the entire volume did not exhibit changes during learning and recall trials (Fig. 3 *C* and *D*). Similar to the formation of context A–related neuronal ensembles, memory

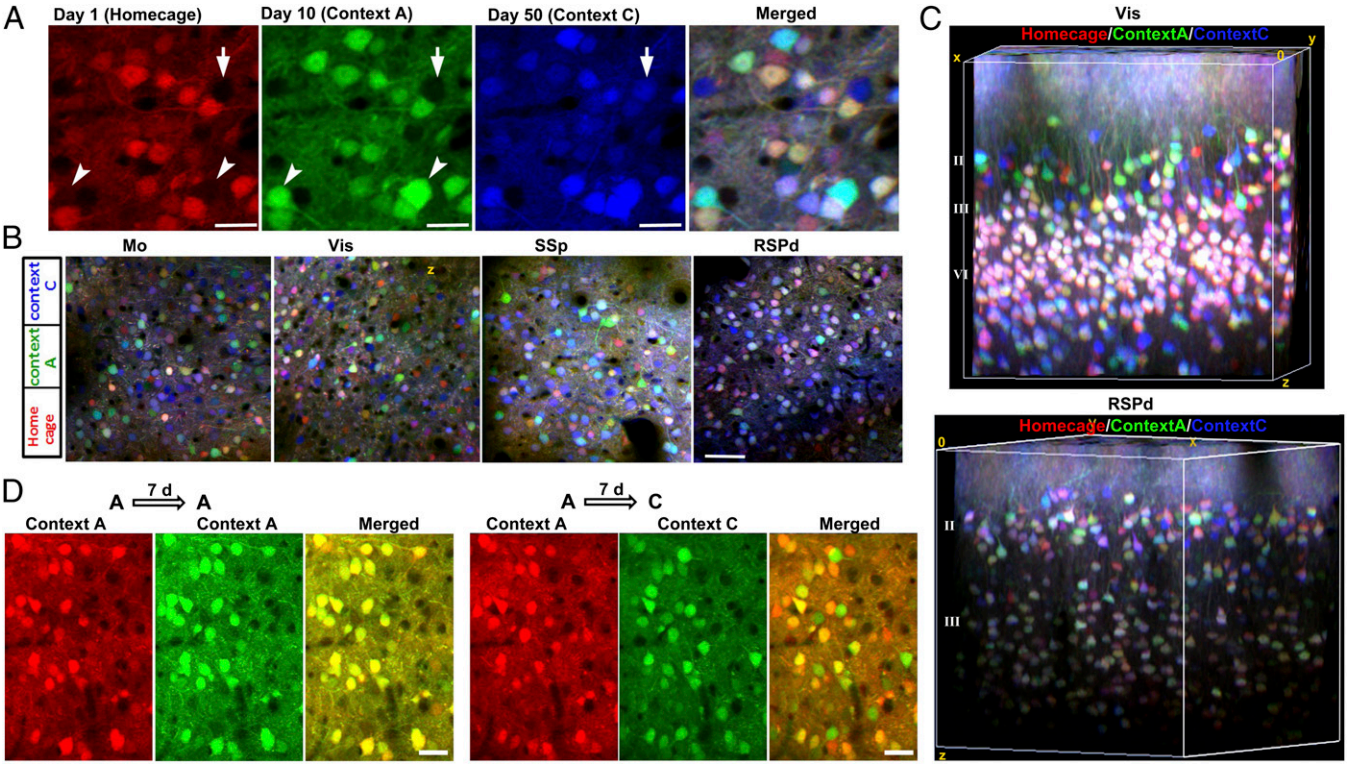

Fig. 2. Tracking of neuronal activation evoked by various tasks within the same cortical volume over 2 mo. (*A*) The visualization of the activity-related EGFP signals induced by three distinct tasks. Intensities of the EGFP signals for each trial are showed under pseudocolor. Mouse was trained in context A on day 10 and context C on day 50. Red, homecage trial; green, context A trial; blue, context C trial. Arrowheads show neurons activated by the context A trial; arrow shows the neuron activated by the context C trial. (Scale bar, 22 μm.) (*B*) The task-specific neuronal activation observed in multiple cortical areas in the same mouse. Red, homecage trial on day 1; green, context A trial on day 10; blue, context C trial on day 50. (Scale bar, 50 μm.) (*C*) 3D reconstructions of the EGR1-EGFP signals induced by three distinct task trials. Red, homecage trial; green, context A trial; blue, context C trial. Visual area and RSPd areas in the same mice were shown. Blocks size, 300 × 300 × 300 μm for Vis, 300 × 300 × 260 μm for RSPd. (*D*) L2 neurons in the visual cortex showed significant difference in activation in the different contexts but not the same context, measured with an interval of 7 d between each two trials. (Scale bar, 25 μm.)

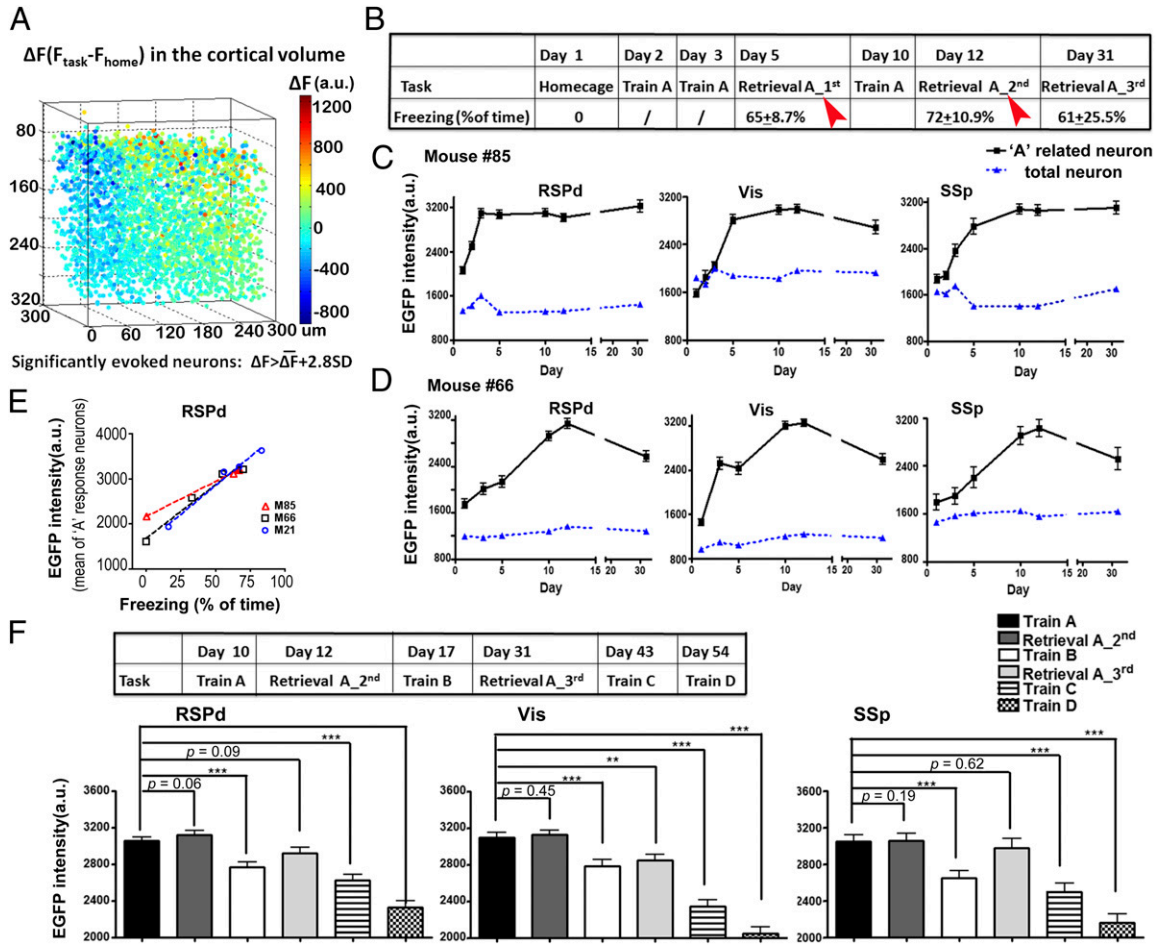

Fig. 3. The formation and maintenance of contextual fear memory-related traces in the cortical circuit. (*A*) One example of training-induced EGFP signal changes in the RSPd volume. Indexed color for each dot represented the signal difference between the context A training trial and the homecage trial (ΔF) of each individual neuron. The task-evoked neurons were defined as ΔF > 2.8-fold SD in all neurons in this volume. (*B*) Experimental procedure to identify the context A-related neuron ensembles in the cortical circuit. Contextual fear condition training trials were performed. The freezing times for each mouse in the retrieval trials were shown in the table ($n = 3$ mice). The context A–related neurons were identified by common groups showed significant task-induced activation in both of the two retrieval trials, indicated as the red arrowhead. (*C*) The formation of memory-related response in multiple cortical regions of one mouse. Neurons showed task-induced activities in both of the recall trials (retrieval A_1st and retrieval A_2nd) were marked as the context A–related trace cells (RSPd, $n = 27$; Vis, $n = 26$; SSp, $n = 36$). The averaged EGFP signals of all neurons in the entire volume were shown in blue line as a control (RSPd, $n = 3{,}420$; Vis, $n = 3{,}926$; SSp, $n = 4278$). (*D*) The formation of context A–related trace cells in another mouse (for A related neurons, $n = 35$ in RSPd, $n = 29$ in Vis, $n = 9$ in SSp; for total neurons, $n = 4{,}274$ in RSPd, $n = 2{,}681$ in Vis, $n = 2{,}826$ in SSp). (*E*) The memory retrieval-induced EGR1-EGFP intensities in the identified memory trace cells was linearly correlated with the freezing time during the trial. The averaged EGFP intensity in the identified memory trace neurons for context A in RSPd volumes was shown (M66, $R^2 = 0.970$ $n = 65$ neurons from three RSPd volumes; M85, $R^2 = 0.999$, $n = 37$ from two RSPd volumes; M21, $R^2 = 0.981$, $n = 10$ from one RSPd volume). (*F*) Context selectivity of the memory trace neurons for the context A. On day 17, mice were trained in context B for contextual fear. On day 43, mice were trained in the context C for passive avoidance. On day 54, mice were trained in the context D for tunnel exploring. The EGFP signals of memory trace neurons in each trial were compared with the context A trial on day 10 ($n \geq 30$ cells from three mice). Paired Student *t* tests were performed. ***$P < 0.001$; **$P < 0.01$; *$P < 0.05$; Error bar, SEM.

traces for context C in the identical cortical area were also gradually formed during training trials for context C in another neuronal ensemble (Fig. S7). The EGR1 expression response to the training context was long lasting. Three weeks after the last training trial, context A continued to evoke a high level of EGFP expression in the memory trace–related neuronal ensembles, suggesting that the activation in these neuronal ensembles may represent the long-term memory (Fig. 3 *C* and *D*).

Importantly, the signal intensities in these sparsely activated neurons in the RSPd volume were correlated with the memory recall. Consistent with the report that the RSP is involved in memory formation in contextual fear tasks (33, 34), the averaged EGFP intensities in the identified neuronal ensembles exhibited a strong linear correlation with the freezing behavior for each recall trial of each individual animal (mouse 66: $R^2 = 0.9699$, $P = 0.015$, $n = 65$ neurons; mouse 85: $R^2 = 0.9986$, $P = 0.0007$, $n = 30$; mouse 21: $R^2 = 0.9810$, $P = 0.0095$, $n = 10$; Fig. 3*E*). These results indicated that the activities in the identified neuronal ensembles in the RSP were related to the recall of contextual fear memory in mice.

To test the context specificity of the EGFP signals in the identified neuronal ensembles, a trial of contextual fear training under context B was performed 5 d after the second recall trial of context A. The EGFP intensities in the task-specific neurons were significantly reduced on context B training in the RSPd ($P = 0.0001$, $n = 80$ cells from three mice), Vis ($P = 0.0007$, $n = 55$ cells from three mice), and SSp areas ($P = 0.0005$, $n = 45$ cells from three mice), indicating the specificity of the context-related neuronal activities in these sensory-related cortical areas (Fig. 3*F*). Similarly, for trials in context C ($P < 0.0001$, in the RSPd, SSp, and Vis) and context D ($P < 0.0001$, in all areas), the identified context A–activated neuronal ensembles exhibited

significant reductions in the EGFP signals (Fig. 3*F*). In contrast to the signal decrease in the context B trial, during the third recall trial for context A, the context-specific neurons exhibited levels of EGFP signals similar to those for training A trial at day 10 (Fig. 3*F*). Therefore, the neuronal ensembles exhibited high levels of EGFP signals that were induced by context A. This high level of expression was not due to the temporal approximation effect. Collectively, these results indicated that the contextual memory traces were gradually formed in the RSPd. Task-specific responses in a small population of neurons were also identified in the Vis and SSp areas, suggesting that contextual fear memory shows distributed organization in various cortical regions.

We further examined the laminar distribution of the identified neuronal ensembles in the cortical volume. By quantifying the percentage of context A–related neurons in each sublayer (depth of 20 μm), we found, surprisingly, that although the EGFP-positive neurons were distributed throughout the volume, the neurons that exhibited significant task-evoked activities were primarily identified in the superficial level of cortical L2/3 in the visual cortex, ∼100 μm below the pia mater (Fig. 4*A*; $n = 17$, cortical volumes from three mice). Such laminar-specific location of context-specific neurons was not due to technical bias, such as spherical aberration. The average cellular EGFP signal intensity in L4 was even higher than that in L2 (Fig. S8). EGR1 expression that was specifically induced by context A occupied up to 5% of the cells in the superficial L2 in the RSPd, Vis, and SSp areas.

To further confirm that the task-induced responses in the cortical volume were layer specific, we compared the task-evoked signal in each neuron within two layers. The superficial layer (L2) consisted of neurons 80–120 μm below the pia mater, whereas the deep layer consisted of neurons 220–260 μm below the pia mater. A comparison of the EGR1 signal in each neuron for two trials in an identical context revealed that the induced EGR1 expression in the two layers exhibited a similar level of variance (Fig. 4 *B* and *C*). In contrast, a comparison of the induced EGR1 signal when the mouse was exposed to a different context revealed that the layer II neurons exhibited a significantly greater variance than neurons in deep layers (Fig. 4 *D* and *E*), indicating that the task-specific responses were more significant in L2.

The identified task-specific neuronal ensembles for different contexts were separated within superficial cortical L2/3. By plotting each neuronal ensemble (ΔF > 2.8-fold of the SD) in layer II, we found very little overlap, indicating that different context-related representations were separated as topographic maps in the cortex (Fig. 4 *F* and *G* and Fig. S9). The traces for one task were sparsely located. The neuronal ensembles for different tasks were intermingled with each other in cortical layer II.

Discussion

Similar to a previous report (16), we report herein that the multiphoton imaging of immediate early gene signals in cortical circuits was able to reveal information representation in the whole local volume of the cortex. The enhanced signal in the EGR1-EGFP mice and a newly developed algorithm to automatically detect EGFP-positive neurons enabled us to monitor and compare greater numbers of neurons within a local cortical circuit over a long time to record behavior-associated neuronal activity changes using a high-throughput analysis.

The expression of EGR1 correlates with neuronal activation, particularly with high-frequency spiking (26, 27). The stability of the reporter protein leads to the accumulation of activity-induced signals within a period. Therefore, the EGFP signal reflects the convolution of neuronal activation rather than single spike events at a specific time point. This feature of IEG-mediated imaging may be useful to quantify the cellular activation that occurs during a behavioral task, in which external stimuli vary from time to time within a specific context, to search for task-specific but not stimuli-specific responses. The finding of context specific responses in superficial layers is consistent with an early report (35). Long-term tracking revealed context-specific changes in IEG expression in L2 neurons within all observed cortical circuits, indicating cortex-wide integration and discrimination of different memory traces.

Similar to the concept that EGFP signals indicate the convolution of neuronal activation, the nonseparated signals in most of the neurons, particularly in L3 and L4, did not suggest that different contexts induced similar neuronal activities in these cells. Instead, these overlapping signals in L3/4 reflected the temporal integration of various stimuli-induced activations during the task period in free-moving mice. This explanation was further confirmed by the finding that simple visual stimuli could induce significantly different EGFP signals in L3 and L4 neurons in anesthetized reporter mice (Fig. S10). Therefore, the apparent lack of signal changes in L3 and L4 neurons in different contexts suggests that the L3 and L4 neurons processed the elementary signals, which are commonly shared in different contexts in free-moving mice.

Our pilot experiments imaged the formation process of these sparse coding neurons in the cortex. In contrast to the rapid

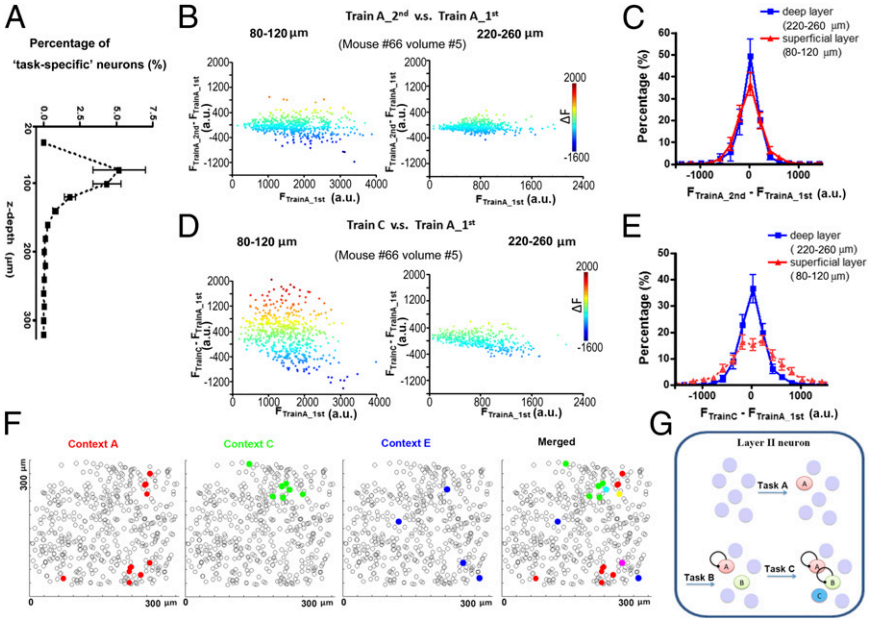

Fig. 4. Localization of context-specific memory traces in L2 neurons. (*A*) The quantification of the dorsal-ventral distribution (*z* axis) for identified memory trace cells in 17 cortical volumes from three mice. Cells in each volume were divided into subgroups along the *z* axis at 20 μm/layer. (*B* and *C*) The EGFP signal difference between two training trials under context A. Each point showed the signal in each neuron. Quantification showed few differences between the superficial layer and deep layer ($n = 4$ RSPd volumes from three mice). (*D* and *E*) The EGFP signal difference between the training trials under context A and context C. Significant changes were seen only in the superficial layer ($n = 4$ RSPd volumes from three mice). (*F*) The distribution of memory traces for different contexts in L2. All neurons (within 120 μm below pia mater) were marked with black circle. Identified memory traces for different contexts were marked with different colors. Few neurons showed response to two contexts. (*G*) Summarized model for the separation of different memory traces during learning. New memories for new contexts could form traces in naive neurons.

formation of memory-related responses of place cells in the hippocampal circuit (1, 21), the observed context-specific responses in the cortical circuit were formed several days after training, suggesting the slow emergence of the memory traces as a long-term process in the cortical circuit. These observations are consistent with the hypothesis that remote memories are slowly consolidated into the neocortex (4, 5, 36).

Finally, the in vivo imaging system using the EGR1-EGFP reporter demonstrated promising features that enabled us to perform repeatable and robust long-term recordings on a large number of neurons over months. This system provides a tool to quantitatively evaluate behavioral task–induced responses and modifications in the cortical circuit to allow the monitoring of the learning-induced changes in the cortical circuits (5, 36) under natural and experimental conditions.

Materials and Methods

In Vivo Imaging of Neuronal Activity. The mouse strain was BAC-EGR-1-EGFP [Tg(Egr1-EGFP)GO90Gsat/Mmucd, from Gensat project, distributed from Jackson Laboratories]. Animal care was in accordance with the Institutional Guidelines of Tsinghua University. Three- to 5-mo-old mice received cranial window implantation as previously described (32) and recordings began 1 mo later. To implant the cranial window, the mouse was immobilized in custom-built stage-mounted ear bars and a nosepiece, similar to a stereotaxic apparatus. A 1.5-cm incision was made between the ears, and the scalp was reflected to expose the skull. One circular craniotomy (about 6 mm in diameter) was made using a high-speed drill, and a dissecting microscope was used for gross visualization. A glass coverslip (8 mm in diameter) was attached to the skull using dental cement. The space between the coverslip and cortical surface was filled with PBS before sealing. The sterile technique was critical to prevent the infection of the bone. The mice were allowed to recover for 4 wk after surgery. For surgeries and observations, mice were anesthetized with 1.5% (vol/vol) isoflurane. The preparation for imaging was restricted to 20 min after anesthetization for each test. The mice were anesthetized 40 min after training and subjected to optical imaging. Six cortical volumes were recorded during each imaging session within 60 min. The same sets of volumes were measured after different training trials to track neuronal EGFP signals in the same neurons at different training sessions. During imaging, a wax ring was placed on the edges of the coverslip of the cortical window and filled with distilled water to create a well for water immersion lens. EGFP fluorescence intensity (FI) was imaged with an Olympus Fluoview 1000MPE with prechirp optics and a fast acousto-optic modulator mounted on an Olympus BX61WI upright microscope, coupled with a 2-mm working distance, 25× water immersion lens (numerical aperture, 1.05). A mode-locked titanium/sapphire laser (Tsunami; Spectra-Physics) generated two-photon excitation at 920 nm, and three photomultiplier tubes (Hamamatsu) collected emitted light in the range of 380–480, 500–540, and 560–650 nm. The output power of the laser was maintained at 1.56 W, and the power reaching the mouse brain ranged from 7.8 to 12.5 mW. For each cortical volume, the laser power was consistent during the time-lapse images under multitasks. Images were acquired at 2 s/frame at a resolution of 512 × 512 pixels. Stack of images were taken at 2-μm intervals for 150–250 frames. On each session, a field of view was selected according to the marked blood vessel to perform the repetitive imaging on the same volume. To facilitate the location of cortical volumes from section to section, dextran Texas red (Dex Red; 70,000 molecular weight; Invitrogen) was injected into a lateral tail vein to create a fluorescent angiogram, as previously described (32).

Imaging Data Analysis and Quantification. The stack images were aligned with 3D Slicer 3.0 (www.slicer.org; NA-MIC) to correct the position shift of each neuron during imaging. The stack images were further quantified with MatLab (The MathWorks). The 3D volume view was created using Image-J (National Institutes of Health). The center position of the detected neurons was created automatically through the computer-based recognition and further validated manually (*SI Materials and Methods*). The EGFP intensity in each cell for each trial was quantified around the cell center as the averaged intensity in a 12 × 12 × 6-μm voxel. Data analysis was performed with the custom-written code in MatLab. See *SI Materials and Methods* for more details. Data are presented as mean ± SEM.

ACKNOWLEDGMENTS. We thank Guosong Liu, Minmin Luo, Gao Hua, Xiaoke Chen, Zhong Yi, and Zhang Xu for advice and critical comments on our manuscript. The work is supported by National Basic Research Program of China Grant 2013CB835100, National Natural Science Foundation of China (NSFC) Grant 31171008 (to J.-S.G.), Tsinghua University Grant 2011Z02143 (to J.-S.G.), and NSFC Grant 31100776 (to H.X.). J.-S.G. is an Investigator of the Center for Life Sciences.

1. Liu X, et al. (2012) Optogenetic stimulation of a hippocampal engram activates fear memory recall. *Nature* 484(7394):381–385.
2. Squire LR, Stark CE, Clark RE (2004) The medial temporal lobe. *Annu Rev Neurosci* 27: 279–306.
3. McGaugh JL (2000) Memory—A century of consolidation. *Science* 287(5451):248–251.
4. Wiltgen BJ, Brown RA, Talton LE, Silva AJ (2004) New circuits for old memories: The role of the neocortex in consolidation. *Neuron* 44(1):101–108.
5. Frankland PW, Bontempi B (2005) The organization of recent and remote memories. *Nat Rev Neurosci* 6(2):119–130.
6. Sacco T, Sacchetti B (2010) Role of secondary sensory cortices in emotional memory storage and retrieval in rats. *Science* 329(5992):649–656.
7. Georgopoulos AP, Schwartz AB, Kettner RE (1986) Neuronal population coding of movement direction. *Science* 233(4771):1416–1419.
8. Chen X, Gabitto M, Peng Y, Ryba NJ, Zuker CS (2011) A gustotopic map of taste qualities in the mammalian brain. *Science* 333(6047):1262–1266.
9. Jarosiewicz B, et al. (2008) Functional network reorganization during learning in a brain-computer interface paradigm. *Proc Natl Acad Sci USA* 105(49):19486–19491.
10. Santhanam G, Ryu SI, Yu BM, Afshar A, Shenoy KV (2006) A high-performance brain-computer interface. *Nature* 442(7099):195–198.
11. Nicolelis MA (2003) Brain-machine interfaces to restore motor function and probe neural circuits. *Nat Rev Neurosci* 4(5):417–422.
12. Stosiek C, Garaschuk O, Holthoff K, Konnerth A (2003) In vivo two-photon calcium imaging of neuronal networks. *Proc Natl Acad Sci USA* 100(12):7319–7324.
13. Svoboda K, Denk W, Kleinfeld D, Tank DW (1997) In vivo dendritic calcium dynamics in neocortical pyramidal neurons. *Nature* 385(6612):161–165.
14. O'Donovan MJ, Ho S, Sholomenko G, Yee W (1993) Real-time imaging of neurons retrogradely and anterogradely labelled with calcium-sensitive dyes. *J Neurosci Methods* 46(2):91–106.
15. Wachowiak M, Cohen LB (2001) Representation of odorants by receptor neuron input to the mouse olfactory bulb. *Neuron* 32(4):723–735.
16. Wang KH, et al. (2006) In vivo two-photon imaging reveals a role of arc in enhancing orientation specificity in visual cortex. *Cell* 126(2):389–402.
17. Barth AL (2007) Visualizing circuits and systems using transgenic reporters of neural activity. *Curr Opin Neurobiol* 17(5):567–571.
18. Barth AL, Gerkin RC, Dean KL (2004) Alteration of neuronal firing properties after in vivo experience in a FosGFP transgenic mouse. *J Neurosci* 24(29):6466–6475.
19. Rakhade SN, et al. (2007) Activity-dependent gene expression correlates with interictal spiking in human neocortical epilepsy. *Epilepsia* 48(Suppl 5):86–95.
20. Dragunow M, Faull R (1989) The use of c-fos as a metabolic marker in neuronal pathway tracing. *J Neurosci Methods* 29(3):261–265.
21. Reijmers LG, Perkins BL, Matsuo N, Mayford M (2007) Localization of a stable neural correlate of associative memory. *Science* 317(5842):1230–1233.
22. Han JH, et al. (2009) Selective erasure of a fear memory. *Science* 323(5920):1492–1496.
23. Zhou Y, et al. (2009) CREB regulates excitability and the allocation of memory to subsets of neurons in the amygdala. *Nat Neurosci* 12(11):1438–1443.
24. Garner AR, et al. (2012) Generation of a synthetic memory trace. *Science* 335(6075): 1513–1516.
25. Frankland PW, et al. (2006) Stability of recent and remote contextual fear memory. *Learn Mem* 13(4):451–457.
26. Aydin-Abidin S, Trippe J, Funke K, Eysel UT, Benali A (2008) High- and low-frequency repetitive transcranial magnetic stimulation differentially activates c-Fos and zif268 protein expression in the rat brain. *Exp Brain Res* 188(2):249–261.
27. Cole AJ, Saffen DW, Baraban JM, Worley PF (1989) Rapid increase of an immediate early gene messenger RNA in hippocampal neurons by synaptic NMDA receptor activation. *Nature* 340(6233):474–476.
28. Boyden ES, Zhang F, Bamberg E, Nagel G, Deisseroth K (2005) Millisecond-timescale, genetically targeted optical control of neural activity. *Nat Neurosci* 8(9):1263–1268.
29. Zhang F, Wang LP, Boyden ES, Deisseroth K (2006) Channelrhodopsin-2 and optical control of excitable cells. *Nat Methods* 3(10):785–792.
30. Trachtenberg JT, et al. (2002) Long-term in vivo imaging of experience-dependent synaptic plasticity in adult cortex. *Nature* 420(6917):788–794.
31. Mank M, et al. (2008) A genetically encoded calcium indicator for chronic in vivo two-photon imaging. *Nat Methods* 5(9):805–811.
32. Xie H, et al. (2013) Rapid cell death is preceded by amyloid plaque-mediated oxidative stress. *Proc Natl Acad Sci USA* 110(19):7904–7909.
33. Keene CS, Bucci DJ (2008) Neurotoxic lesions of retrosplenial cortex disrupt signaled and unsignaled contextual fear conditioning. *Behav Neurosci* 122(5):1070–1077.
34. Robinson S, Poorman CE, Marder TJ, Bucci DJ (2012) Identification of functional circuitry between retrosplenial and postrhinal cortices during fear conditioning. *J Neurosci* 32(35):12076–12086.
35. Burke SN, et al. (2005) Differential encoding of behavior and spatial context in deep and superficial layers of the neocortex. *Neuron* 45(5):667–674.
36. Sutherland GR, McNaughton B (2000) Memory trace reactivation in hippocampal and neocortical neuronal ensembles. *Curr Opin Neurobiol* 10(2):180–186.